Article:

Jackson, J., Childs, D.Z. orcid.org/0000-0002-0675-4933, Mar, K.U. et al. (2 more authors) (2019) Long-term trends in wild-capture and population dynamics point to an uncertain future for captive elephants. Proceedings of the Royal Society B: Biological Sciences, 286 (1899). 20182810. ISSN 0962-8452

https://doi.org/10.1098/rspb.2018.2810

Supplementary information

Long-term trends in wild-capture and population dynamics point to an uncertain future for captive elephants.

S1. Data selection

The data recorded for all registered elephants includes: identification number and name, birth origin (captive-born or wild-caught), date and place of birth, mother's identification number and name, year and place of capture (if wild-captured), year or age of taming, identities of all calves born, date of death or last known date alive, and cause of death. The initial studbook contained data from 1876 to 2014. Further restrictions to the studbook were made because only sparse records were available until the 1950s. Therefore, only females born after 1920 if captive-born were included, and both mortality and birth records for females present in the population before 1960 were discarded. Records for wild-caught individuals were incomplete before 1951 and age estimates for wild-caught elephants may have lower accuracy after the individuals have achieved full body height (at the age of 25 years in this working population) (Mumby et al. 2015). Therefore, only wild-caught females entering the population after 1951 and caught before the age of 25 (~70% of those captured), were included here to increase the reliability of our age-specific mortality and fertility estimates. Thus, our measure of annual wild-capture rate does not reflect the total number of individuals caught from the wild each year, but instead general trends of wild-capture through time in Myanmar. Nevertheless, the majority of wild-caught elephants were below an estimated age of 25 at capture: during 1951-1999 the median age at capture varied between 8 and 13 years, depending on the method of capture (Lahdenperä et al. 2018), and capturers generally targeted young, healthy-looking individuals which were easier to train than older ones. There was also a female bias in wild-capture, who comprised 60% of wild-caught individuals in the initial studbook. Finally, individuals with erroneous or discontinuous death/departure/birth information were removed (5% of elephants). The final studbook was a female-only dataset (N = 3585, wild-caught = 1215) with individuals from 11 out of the 14 regional divisions of Myanmar, of which 2117 were censored. This female-only dataset was used in all subsequent analyses.

S2. Model selection

We used model selection in order to explore the fit of linear and non-linear explanatory variables on female birth and mortality rates, as well as on the interaction between age, year and birth origin (table S1). We assessed the fit of models incorporating the age and year parameters as 1) linear parametric terms, 2) smoothing terms fitted using thin plate regressions splines (Wood 2003), 3) separate smoothing terms for wild-caught and captive-born females, to capture the interaction between age/year and birth origin, and 4) a tensor product interaction smoothing term, with separate terms for wild-caught and captive-born females, to capture the interaction between all explanatory variables (Wood 2006). Finally, we also explored the fit of models incorporating a linear term for population size in each year, to assess density dependence in life-history traits and whether there was a need to incorporate density dependence in future projections. All models also had a linear parametric term for birth origin, to assess the differences in mean vital rates between wild-caught and captive-born females. Although a previous study found an effect of the time in captivity on survival in this population (Lahdenperä et al. 2018), because we aimed to assess population viability without continued wild capture (after 1995) this was not included in our model selection. All models also had a random effect smoothing term of spatial division group in Myanmar, penalized with a ridge penalty. We had life history records from 11 out of 14 spatial divisions (Ayeyarwady = 878, Bago = 7167, Chin = 1066, Kachin = 7252, Magway = 3322, Mandalay = 11650, Rakhine = 2004, Sagaing = 25713, Shan = 5749, Tanintharyi = 142, Yangon = 356, Unknown= 4984; figure S1). In the analyses, to make sample sizes more comparable we grouped divisions by proximity and elevation: Ayeyarwady, Yangon, Bago, Rakhine, and Tanintharyi regions were all grouped together because of low sample size and their coastal locations. Chin and Shan regions were grouped together because of their similar elevation and low sample sizes. Finally, Magway and Mandalay regions were grouped together because of similar altitude, proximity and low sample size. The best-fit models were selected using the Akaike information criterion (AIC), and where the difference in AIC between the two best models was less than 2, the simpler model with fewer interactions was selected (Akaike 1987, Burnham and Anderson 2004).

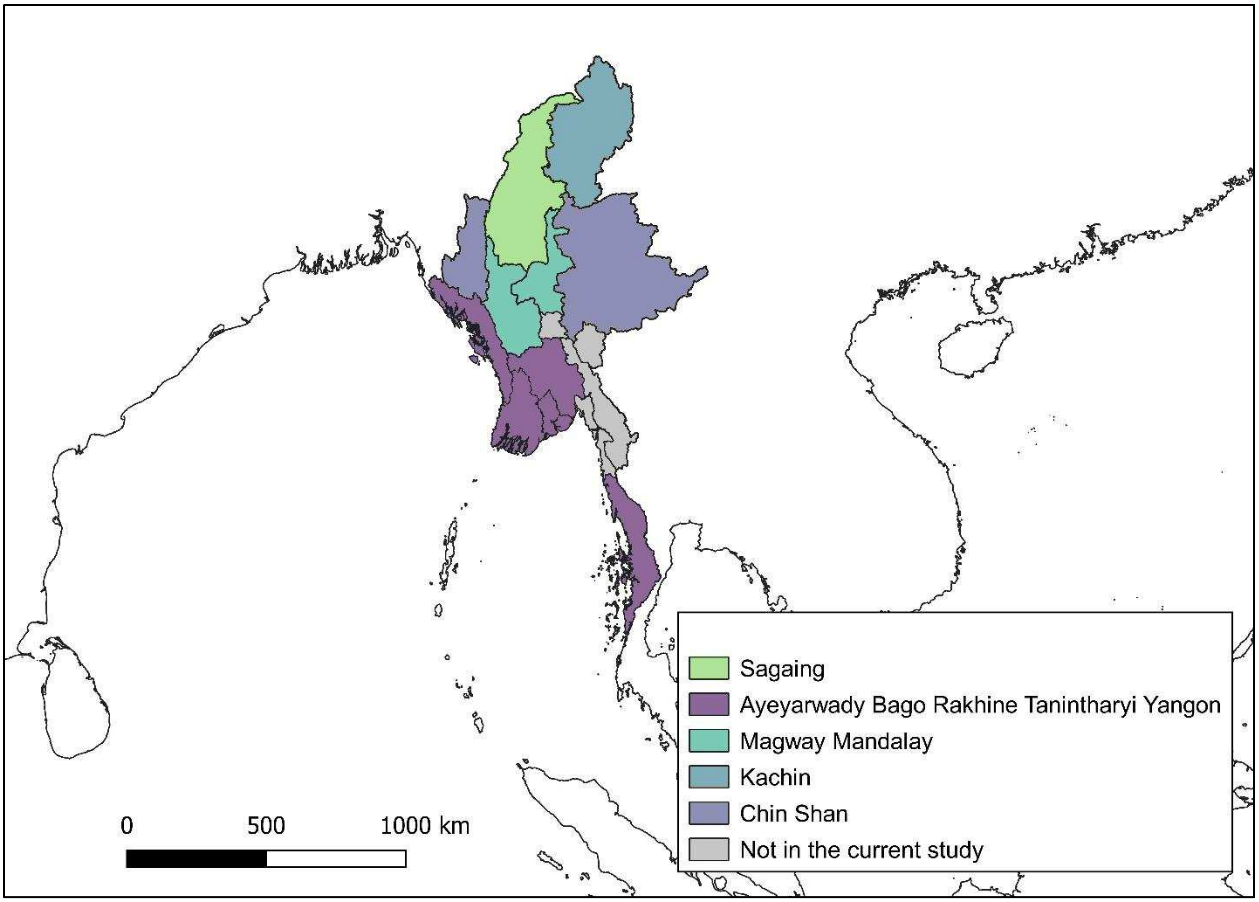

Figure S1. Regional divisions of Myanmar used in the current study. Colour denotes the regional division groups used in analysis.

Table S1. Model selection results for age-specific life-history traits through time in female timber elephants. Best model highlighted in bold. All models also included a binary response variable of birth or mortality, a parametric term for birth origin, and an additional random effect smoothing term predictor for regional division. The function $f(x)$ describes a thin plate regression spline smoother, the function $g(x)$ describes a tensor product interaction smoothing term fit with a thin plate regression spline, and the function $re(x)$ described a random effect smoothing term penalised with a ridge penalty. Terms without functions delineate parametric, linear predictors.

Birth model predictors	AIC	ΔAIC
g(age, year, birth origin = captive-born) + g(age, year, birth origin = wild-caught) + re(year factor)	**12712.61**	
g(age, year, birth origin = captive-born) + g(age, year, birth origin = wild-caught) + population size + re(year factor)	12713.03	0.42
f(year, birth origin = captive-born) + f(year, birth origin = wild-caught) + f(age, birth origin = captive-born) + f(year, birth origin = wild-caught) + re(year factor)	12732.73	20.12
g(age, year, birth origin = captive-born) + g(age, year, birth origin = wild-caught)	12758.12	45.51
f(year, birth origin = captive-born) + f(year, birth origin = wild-caught) + f(age) + re(year factor)	12759.73	47.12
f(year) + f(age, birth origin = captive-born) + f(year, birth origin = wild-caught) + re(year factor)	12764.91	52.31
f(year, birth origin = captive-born) + f(year, birth origin = wild-caught) + f(age, birth origin = captive-born) + f(year, birth origin = wild-caught)	12768.62	56.01
f(year, birth origin = captive-born) + f(year, birth origin = wild-caught) + f(age)	12795.52	82.92
f(year) + f(age, birth origin = captive-born) + f(year, birth origin = wild-caught)	12800.55	87.94
f(year) + f(age)	12863.94	151.34
Half-decade + f(age)	12872.52	159.91
Decade + f(age)	12952.38	239.77
year + f(age)	12987.26	274.65
year + age + year: age	13958.57	1245.96
f(year) + age	14204.45	1491.84
year + age + age: birth origin	14375.57	1662.96
year + age + year: birth origin	14414.02	1701.41
year + age	14415.25	1702.64

Mortality model predictors		
g(age, year, birth origin = captive-born) + g(age, year, birth origin = wild-caught) + re(year factor)	**8807.11**	
g(age, year, birth origin = captive-born) + g(age, year, birth origin = wild-caught) + population size + re(year factor)	8807.49	0.38
f(year, birth origin = captive-born) + f(year, birth origin = wild-caught) + f(age, birth origin = captive-born) + f(year, birth origin = wild-caught) + re(year factor)	8839.35	32.24
f(year) + f(age, birth origin = captive-born) + f(year, birth origin = wild-caught) + re(year factor)	8844.44	37.33
g(age, year, birth origin = captive-born) + g(age, year, birth origin = wild-caught)	8862.64	55.53
f(year, birth origin = captive-born) + f(year, birth origin = wild-caught) + f(age) + re(year factor)	8873.19	66.07
f(year, birth origin = captive-born) + f(year, birth origin = wild-caught) + f(age, birth origin = captive-born) + f(year, birth origin = wild-caught)	8883.63	76.52
f(year) + f(age, birth origin = captive-born) + f(year, birth origin = wild-caught)	8886.88	79.77
f(year, birth origin = captive-born) + f(year, birth origin = wild-caught) + f(age)	8916.00	108.89
Hal-decade + f(age)	8930.60	123.49
f(year) + f(age)	8936.67	129.56
Decade + f(age)	8947.66	140.55
year + f(age)	9004.32	197.21
year + age + year: age	9480.85	673.74
year + age + age: birth origin	9515.23	708.12
f(year) + age	9526.44	719.33
year + age + year: birth origin	9581.47	774.36
year + age	9583.10	775.99

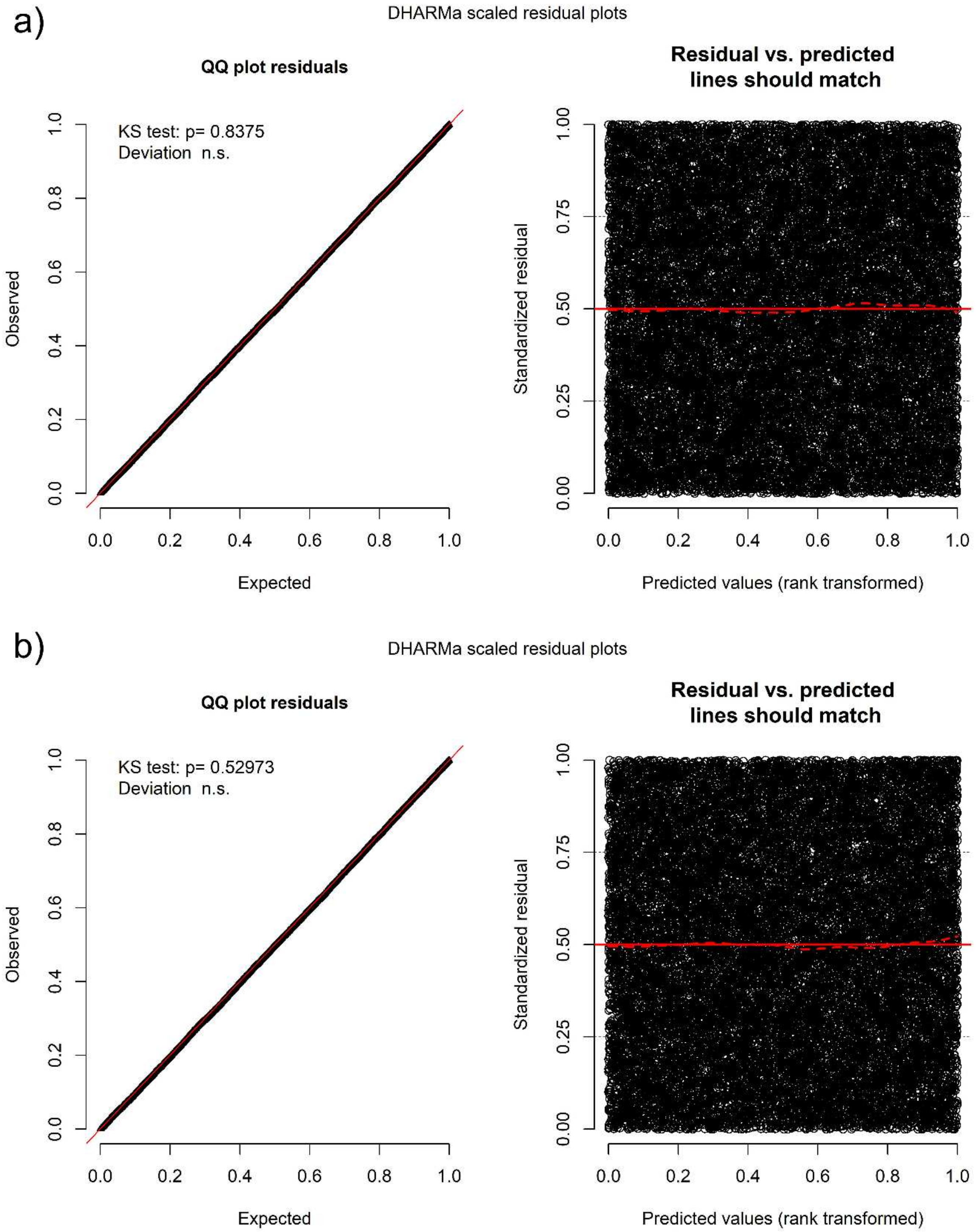

Figure S2. Scaled model residual diagnostics for the best-fit birth (a) and mortality (b) models over 1000 simulations. In neither birth nor mortality models was their evidence for deviation from uniformity in the residuals (left), or a relationship between predicted values and residuals (right).

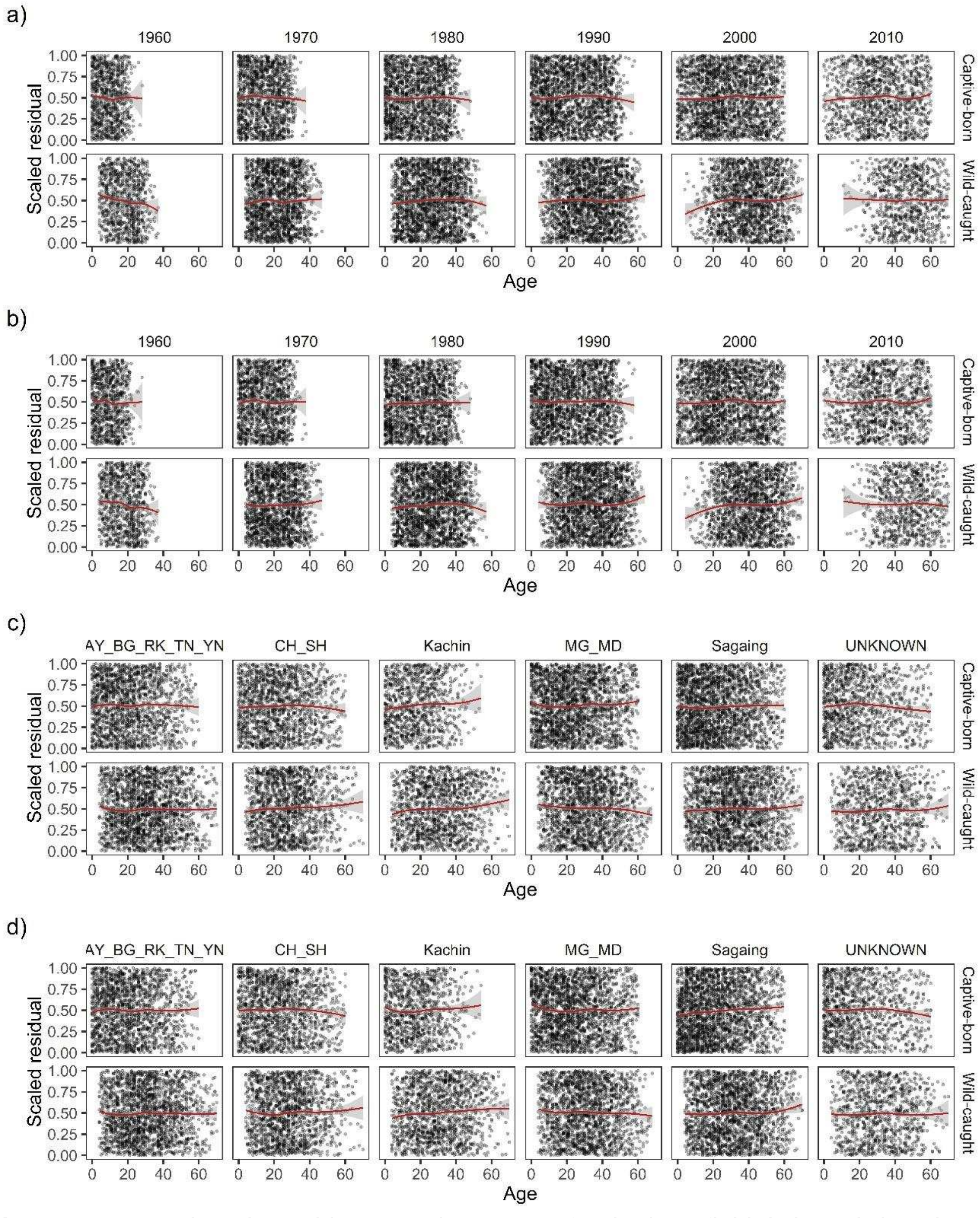

Figure S3. Scaled model residual covariance plots for the best-fit birth (a and c) and mortality (b and d) models. Scaled, simulated residuals were assessed against age, birth origin, decade (a and b) and regional division (c and d). Grouped regional division abbreviations: AY - Ayeyarwady, YN- Yangon, BG - Bago, RK- Rakhine, and TN- Tanintharyi, CH- Chin, SH-Shan, MG- Magway, MD- Mandalay. Points are scaled residuals, red lines are loess (localised regression) smoothers.

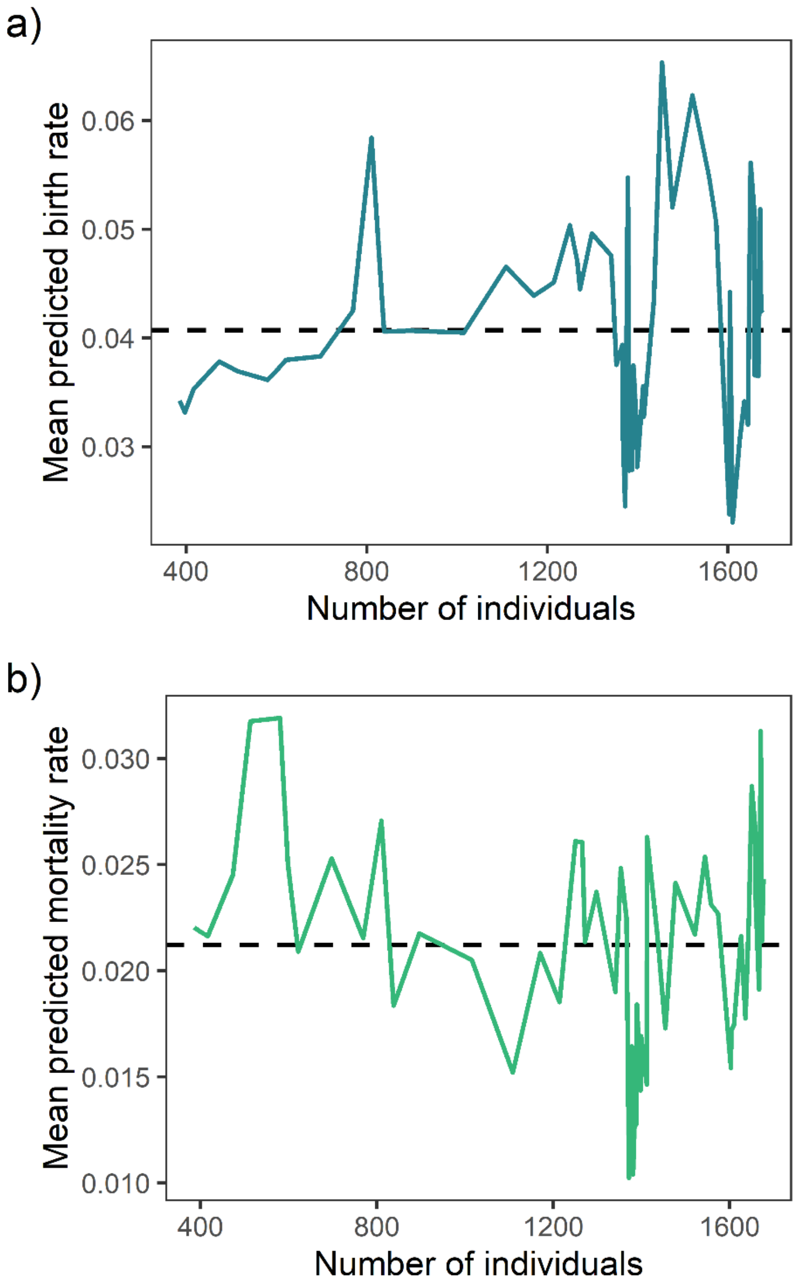

Figure S4 – Mean model predicted values for the best-fit birth (a) and mortality (b) models with respect to population size. Solid lines are mean predicted vital rates, dashed lines are the mean birth and mortality rates across the study period. We found no clear relationship between population size and age-specific vital rates, and no further explanatory power when population size was included in the model (table S1).

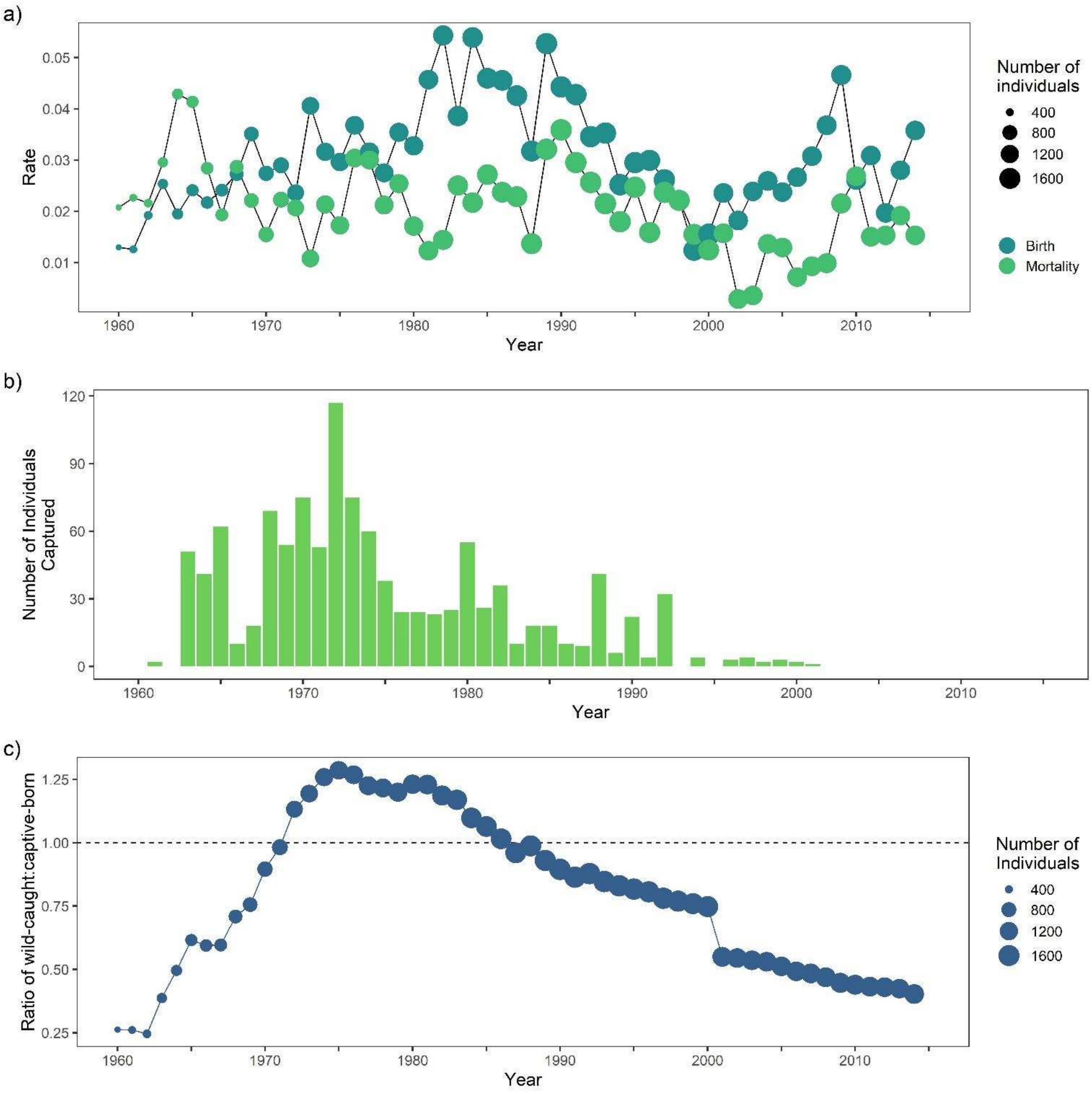

Figure S5. Population trends in female timber elephants between 1960 and 2014. a) Raw annual birth and mortality rates for female timber elephants. The size of the points indicates the population size in each year (range = 385 - 1677). b) Annual capture rate estimates of wild female Asian elephants under the age of 25 in Myanmar between 1960 and 2014. c) The ratio of wild-caught females to captive-born females, where the size of the point indicates the population size (range = 385-1677).

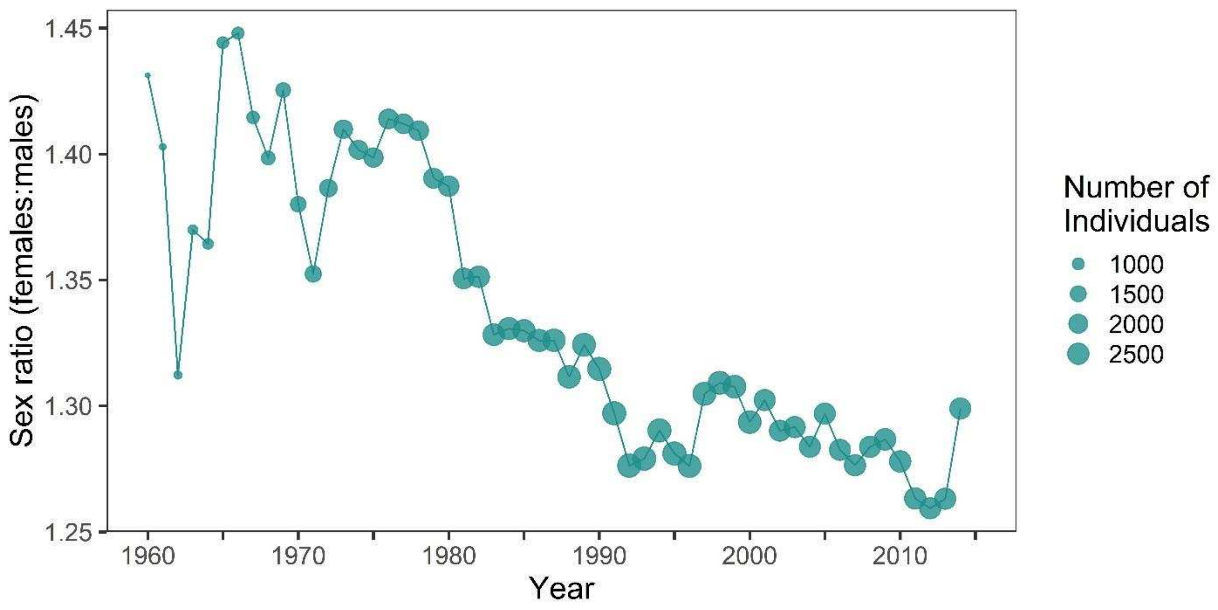

Figure S6. Temporal trend in the sex ratio of timber elephants between 1960 and 2014. The size of the points indicates the population size (range = 654-2991).

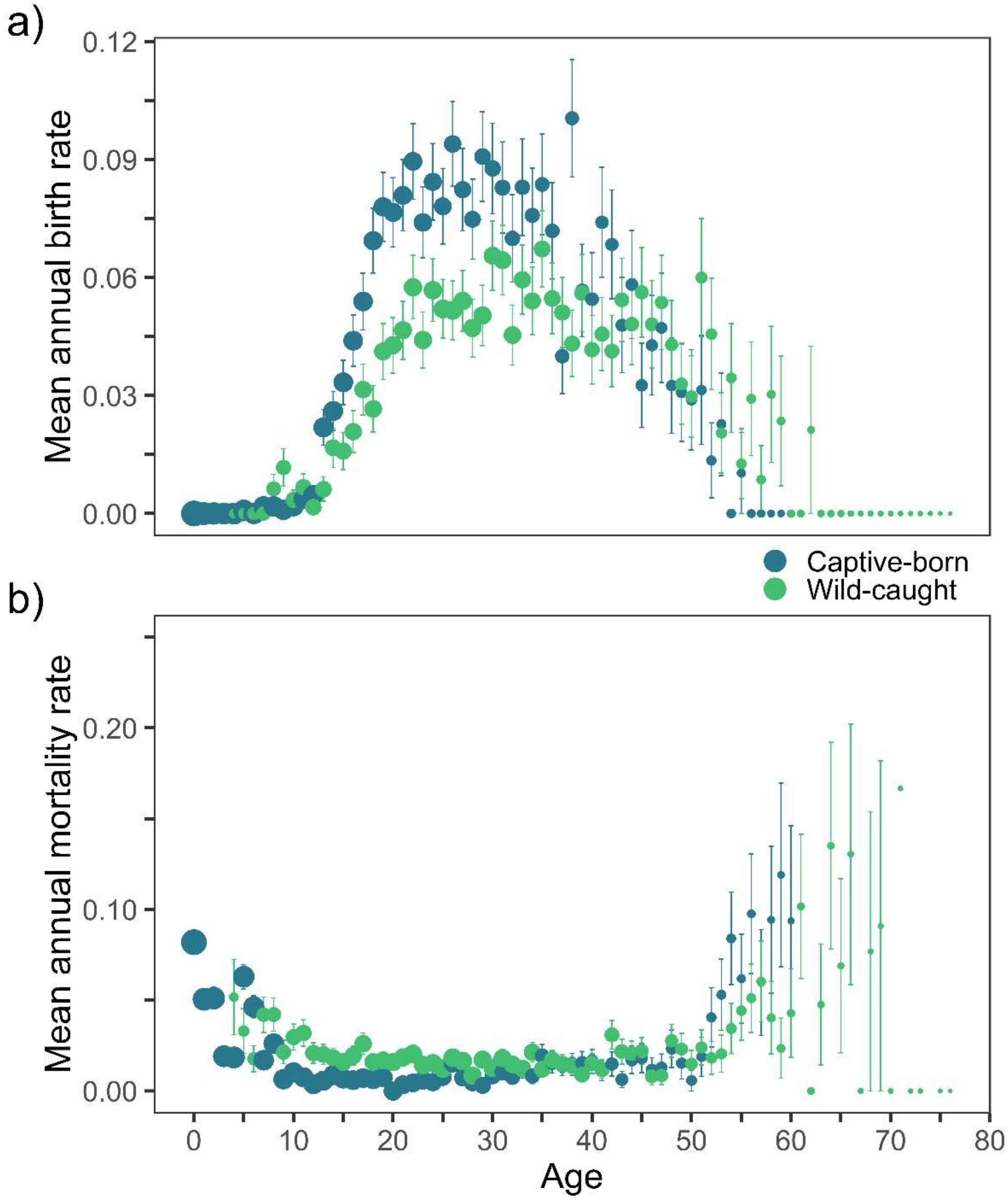

Figure S7. Mean age-specific birth (a) and mortality (b) rates in captive-born and wild-caught female timber elephants between 1960 and 2014. Points are mean annual age-specific birth rates across all years and regional divisions in Myanmar, with standard error bars. The size of the points indicates the sample size for a given age (range = 1-1965).

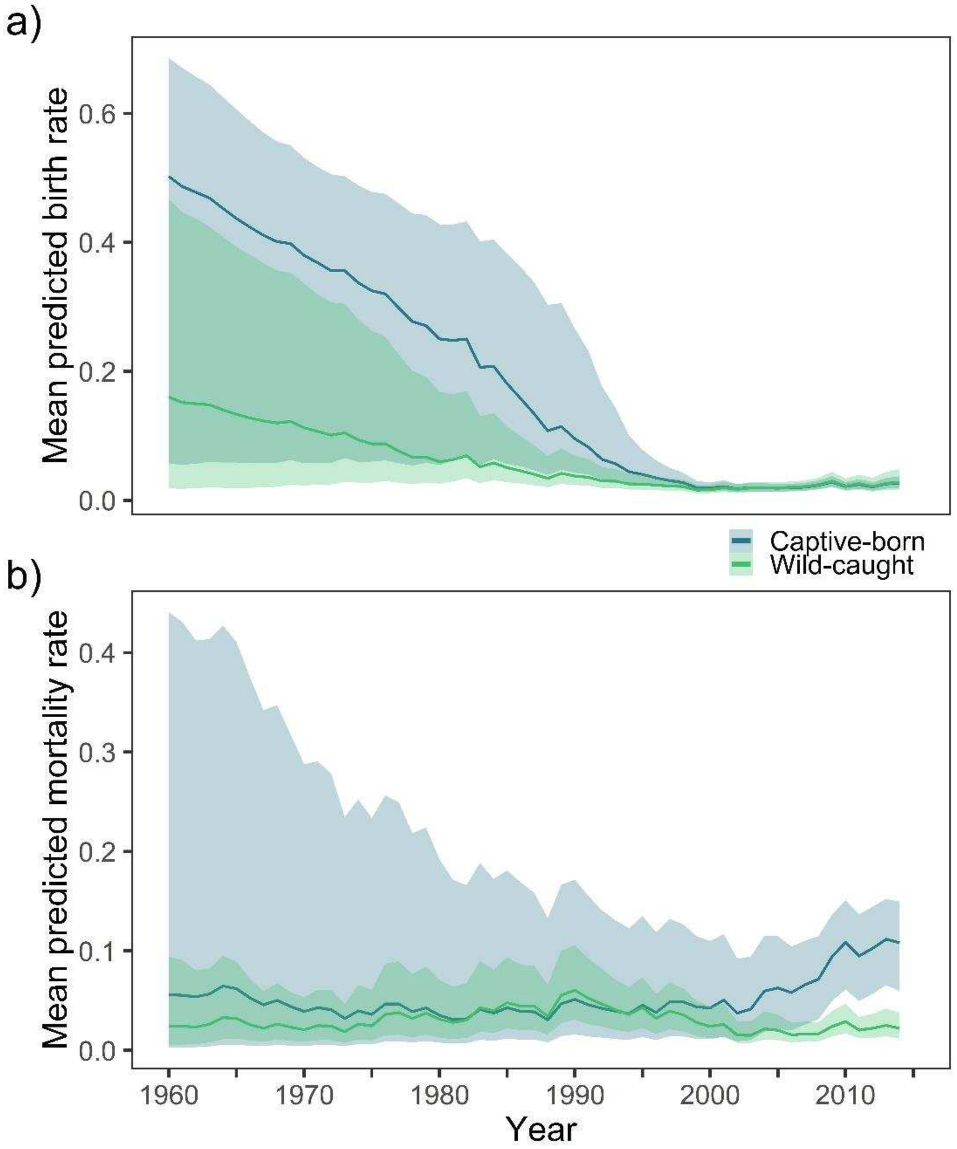

Figure S8. Change in the mean predicted birth (a) and mortality (b) rates between 1960 and 2014 for captive-born and wild-caught females. Lines are mean model predicted values over 1000 posterior simulations with 95% confidence intervals.

S3. Formulation of the stochastic individual-based model

Description of the individual-based model using the ODD protocol described by Grimm et al. 2006.

S3.1 Purpose

The purpose of the model is to understand the long-term population dynamics of captive female elephants in Myanmar in a scenario where wild-capture is no longer practised. Here we present only the formation of the first age-specific projection model, which incorporated only demographic stochasticity and the mean age-specific birth/mortality probabilities across study years (1995-2014) for each birth origin.

S3.2 State variables and scales

The model is formed at the level of each individual female. Individuals are characterised by two state variables: Their age (a, integer between 0 and 70 in years) and their birth origin (captive-born C, or wild-caught W). The population is characterised by the number of individuals in a given year (at each age and of each birth origin).

S3. 3 Process overview and scheduling

The model proceeds in annual time steps. Within each year or time step, 2 phases are processed in the following order: birth and mortality. This order was selected in order to allow females to reproduce and die in the same year. In each year, based on their age and birth-origin, females had a given probability of reproduction or mortality. An overview of the life-cycle and transition probabilities is given in figure S9.

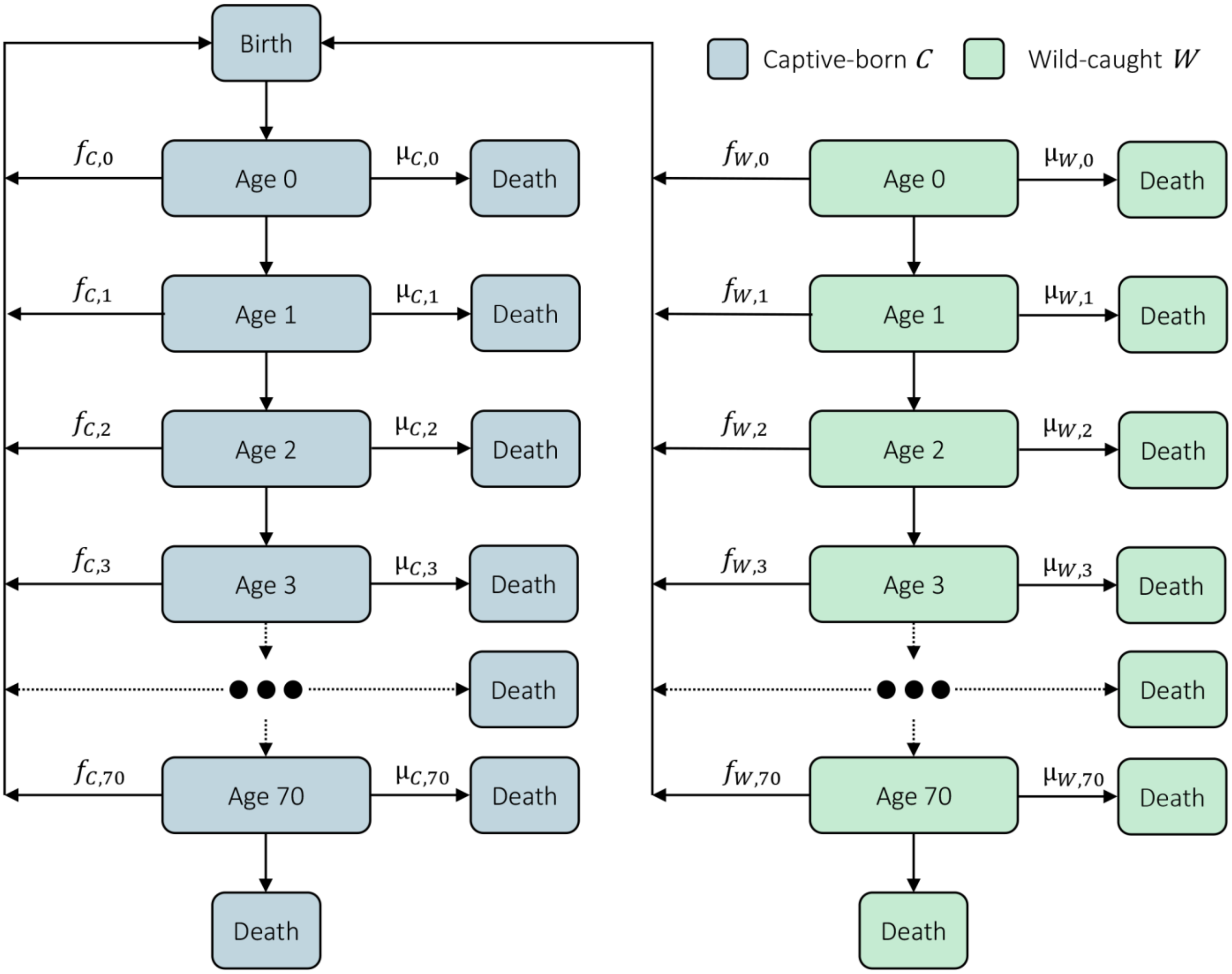

Figure S9. A schematic of the life-cycle for the individual-based stochastic projection model for female timber elephants without wild-capture. Colour denotes birth origin. Each individual at each age (a) had mean annual predicted birth probabilities of $f_{C,a}$ (captive-born) and $f_{W,a}$ (wild-caught), and mean annual predicted mortality probabilities of $\mu_{C,a}$ (captive-born) and $\mu_{W,a}$ (wild-caught). All individuals born were captive-born females at age 0. Individuals living past the age of 70 were removed from the analysis.

S3. 4 Design concepts

Stochasticity: Birth and mortality are interpreted as binary events drawn from the Bernoulli distribution for each individual from each birth origin, with a probability from the mean age-specific probability from the best-fit birth and mortality models. Observation: For model analysis, we recorded the population-level variable of $\ln population\ size$.

S3. 5 Initialization and input

We began the projection with the age-structure present in 2014 (N = 1369), which had 976 captive-born females and 393 wild-caught females. The starting age-structure is given in figure S11. Demographic stochasticity was incorporated by performing 500 iterations of the projection model. We projected forward 250 years, which captured long-term trends over 10-12.5 generations. For this projection, age-specific birth and mortality probabilities were averaged across the study period (1995-2014) from the best-fit model predictions. Furthermore, the projection was run on predicted values from the Kachin regional division. Explicitly, the mean age-specific predicted birth probability, $p(birth)$, is given by the following binomial additive model

$$p(birth) = \left[1 + e^{-(\beta_0 + g(a,\ C) + g(a,\ W))}\right]^{-1}$$

Where β_0 is the intercept, and the function $g()$ describes a tensor product interaction smoothing term fit with a thin plate regression spline for an individual at age a, and separately for captive-born, C, and wild-caught, W, females, but averaged across years 1995-2014, rather than incorporating an observation year effect (table S1). The mean age-specific predicted mortality probability, $p(mort)$, is given by the following binomial additive model

$$p(mort) = \left[1 + e^{-(\beta_0 + g(a,\ C) + g(a,\ W))}\right]^{-1}.$$

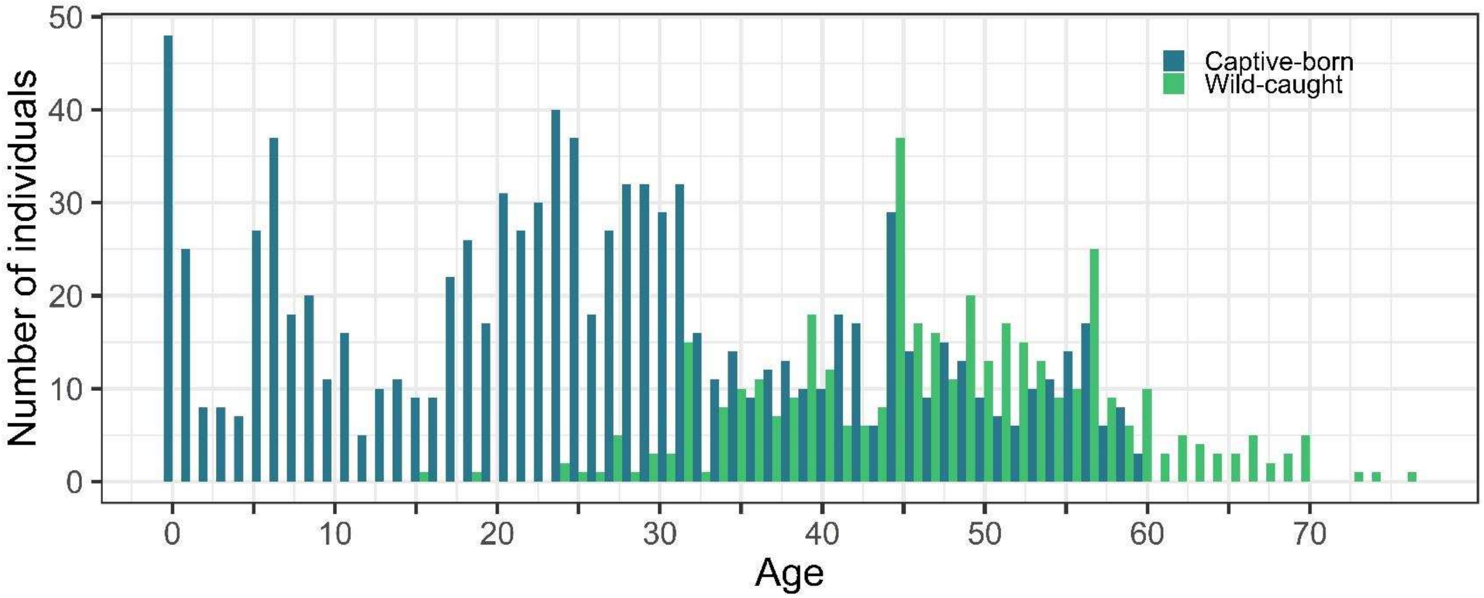

Figure S10. A histogram of the starting age-structure for stochastic, individual-based population projections, which was the age-structure present in 2014 (N = 1369). Ages are in 1-year bins. Colour denotes the birth origin.

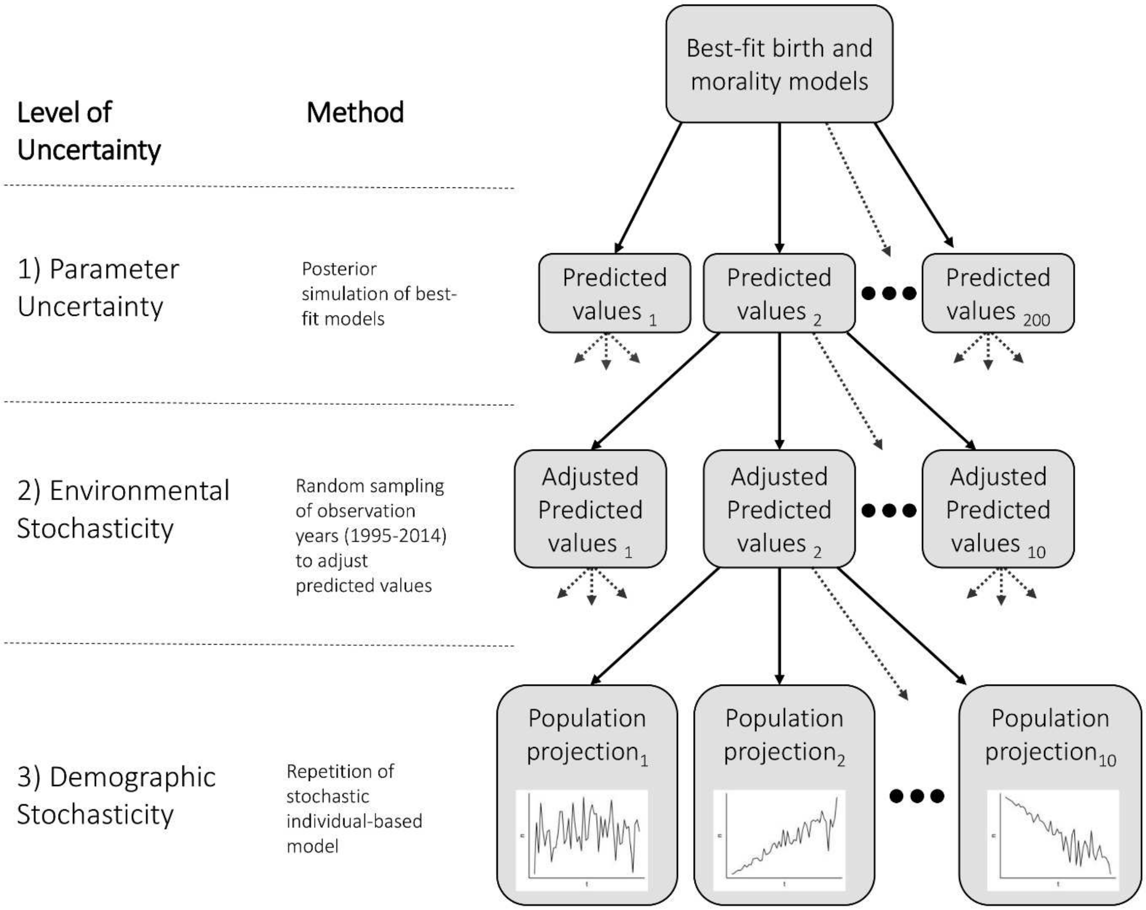

Figure S11. A schematic of the simulation framework for implementing the hierarchical population viability analysis under different levels of uncertainty. Starting from the best-fit birth and mortality models, 1) parameter uncertainty was incorporated through posterior simulation, generating 200 sets of predicted values. 2) Environmental stochasticity was incorporated by randomly sampling 10 sets of years (1995-2014) and adjusting predicted values based on observed variation in those years. 3) Demographic stochasticity was incorporated by repeating each population projection 10 times. When partitioning the variance in $\ln population\ size$ to these three levels of uncertainty, for each year we incorporated the hierarchical framework of demographic stochasticity within environmental stochasticity within parameter uncertainty using nested intercept-only random effects.

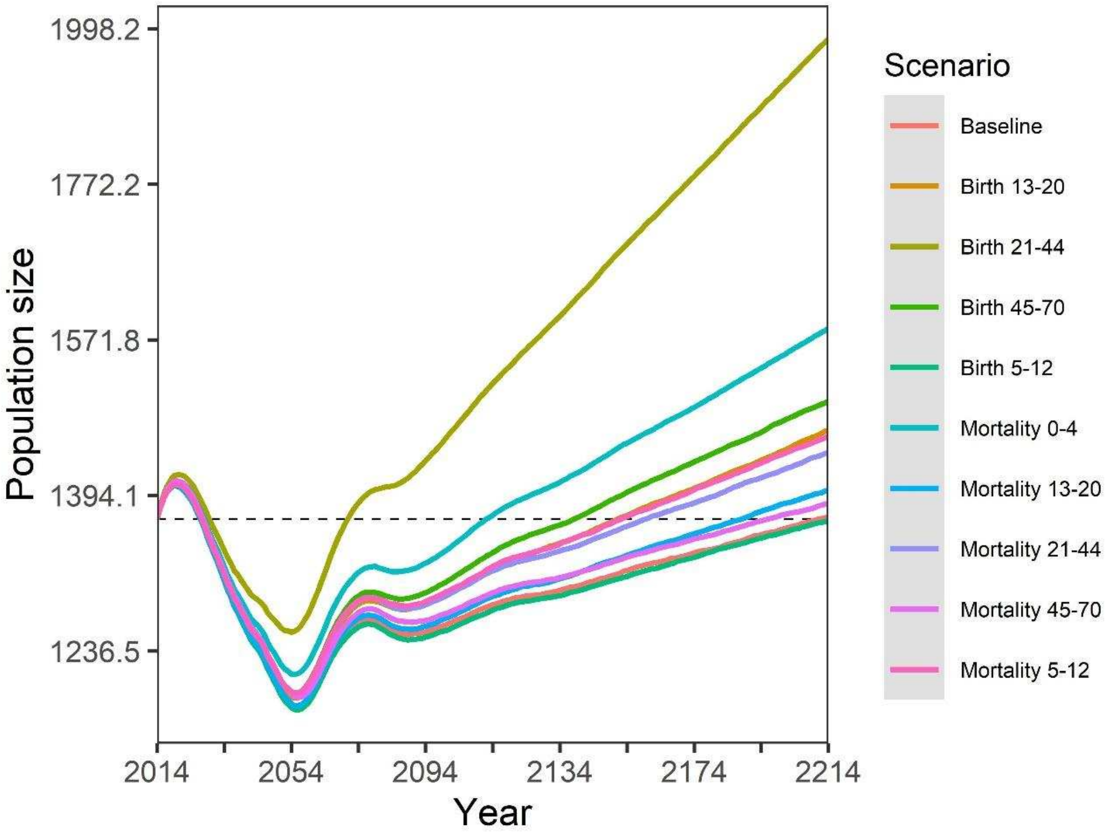

Figure S12. All scenarios of demographic change and their influence on population viability over 200 years. Each line represents either the baseline, average scenario of long-term viability or a scenario with a 10% increase (birth rates) or 10% decrease (mortality rates) for specific age classes. Population size axis on the natural logarithmic scale, dashed line represents starting population size.